ELSEVIER

1 May 1999

Optics Communications 163 (1999) 38–43

OPTICS COMMUNICATIONS

Prismless diode-pumped mode-locked femtosecond Cr:LiSAF laser

A. Robertson [a,*], U. Ernst [a], R. Knappe [a], R. Wallenstein [a], V. Scheuer [b], T. Tschudi [b], D. Burns [c], M.D. Dawson [c], A.I. Ferguson [c]

[a] *Universität Kaiserslautern, Fachbereich Physik, 67653 Kaiserslautern, Germany*
[b] *Technische Hochschule Darmstadt, Institut für Angewandte Physik, 64289 Darmstadt, Germany*
[c] *Institute of Photonics, University of Strathclyde, Glasgow G4 ONG, UK*

Received 26 January 1999; received in revised form 17 March 1999; accepted 17 March 1999

Abstract

A diode-pumped saturable Bragg reflector (SBR) mode-locked Cr:LiSAF laser is demonstrated which requires only a single Gires–Tournois interferometer (GTI) mirror for dispersion compensation. This extremely compact laser produced stable 94 fs pulses with an output power of 110 mW at a wavelength of 848 nm when pumped by 660 mW of light from two broad area red diode lasers.

Keywords: Cr:LiSAF laser; Gires–Tournois interferometer mirror; Saturable Bragg reflector

1. Introduction

The recent years have seen several important advances in both ultra-short pulse sources and applications. Both pico- and femtosecond laser systems have enabled the development of powerful and versatile measurement techniques. In particular, the production of THz radiation for spectroscopy and imaging [1], as well as bio-medical imaging techniques such as two-photon fluorescence [2] and optical tomography [3], have shown great promise as applications which should find use in many areas of science, engineering, and medicine. However, to allow the transition of such tools from the scientific laboratory to the real world, there is a requirement to replace current, large frame based mode-locked systems with compact, low-cost, user-friendly sources. In this contribution, we report on a prismless, femtosecond, diode-pumped, Cr:LiSAF laser which fulfils these criteria. We show that through careful dispersive mirror design and manufacture, only one GTI mirror is required to provide enough negative dispersion for femtosecond, mode-locked operation.

There has been much effort directed in the field of directly diode-pumped femtosecond laser systems. The most promising materials have been the laser active colquiriites, Cr:LiSAF [4] and Cr:LiSGAF [5]. Both possess a wide fluorescence bandwidth essential for the production of fs pulses, as well as having absorption in the red, making them amenable to optical pumping with AlGaInP laser diodes. Of these materials, only Cr:LiSAF can be grown in high enough quality in large volumes. Fs operation of diode-pumped Cr:LiSAF lasers has been reported using the techniques of Kerr lens mode-locking (KLM) [6] and saturable absorber mode-locking (SAM) using either antiresonant Fabry–Perot saturable absorber (A-FPSA) or saturable Bragg reflector (SBR) structures [7,8]. The former technique has the advantage that the optical Kerr effect is non-resonant, allowing mode-locking over a very wide tuning range [9], however, often an external starting technique is required such as a moving mirror, or an electro-optic modulator.

* Corresponding author. Tel.: +49-631-2017-407; Fax: +49-631-2053-906; E-mail: roberts@rhrk.uni-kl.de

0030-4018/99/$ - see front matter
PII: S0030-4018(99)00145-5

Mode-locking using intracavity semiconductor saturable absorbers has proven very successful with diode pumped systems. They are compact, can be designed to operate in a wide spectral range, are relatively alignment-insensitive and potentially very inexpensive. Another major benefit of the absorber is an improvement in self-starting properties of the mode-locking. However, unlike the Kerr effect, the saturable absorber is a resonant device, and wavelength tunability is limited, depending on the exact structure of the absorber. The most simple absorbers offer 10 nm or less tunability while more complicated designs have been reported which offer a tunability of up to 50 nm [10].

A further important development has been a rapid advance in the successful implementation of low loss dispersion compensating mirrors in the form of either Gires–Tournois interferometer (GTI) [11] or chirped mirrors (CM) [12]. The advantages offered by all-mirror resonators over prism-based systems are significant, especially for the development of compact, robust systems. The elimination of intra-cavity prisms enables the design of shorter resonators as there is no longer the restraint of a required prism separation. The use of high refractive index material for prisms does reduce the prism separation but at the expense of increased absorption losses, which are extremely detrimental to the performance of low gain Cr:LiSAF material. Finally, less overall cavity elements lead to the additional benefits of lower losses and increased cavity stability. The GTI has been used successfully for dispersion compensation in both the picosecond [13] and the femtosecond [14] regime.

The use of GTI mirrors has been intensively investigated in mainframe krypton laser pumped KLM Cr:LiSAF and Cr:LiSAGaF systems [15]. A diode pumped KLM system has also been reported which produced 55 fs pulses but with an average output power of only 20 mW [16]. Also, a diode-pumped, femtosecond Cr:LiSAF laser was demonstrated which used a semiconductor saturable absorber mirror with dispersion compensation, based on a Gires–Tournois structure [17]. This laser produced 25 mW of average output power with pulses of 160 fs duration. However, scaling to higher powers resulted in unstable mode-locking and shorter pulse durations could not be achieved because the semiconductor device could not provide dispersion compensation over a broader spectrum. A KLM diode pumped femtosecond Cr:LiSGAF laser has also been reported in which CM were used [18]. For optimum dispersion compensation, this system required sixteen bounces per round trip on the CM.

By combining the advantages of mirror dispersion compensation, diode pumping, and saturable absorber mode-locking, we have designed and investigated the performance of a compact, stable, femtosecond system. Dispersion compensation was provided by a single GTI mirror, resulting in an extremely simple cavity design with high stability and very low losses. We believe this laser to be ideal for use as a turn-key oscillator in, for example, THz production, biomedical imaging or as a seed laser for further amplification.

2. Mirror design

The GTI is an etalon with ideally 100% reflection from the back surface and a small reflection from the front surface. A GTI can be made very simply by the addition of a weak cavity to the front of a nominally high reflecting dichroic mirror constructed of quarterwave stacks of materials of different refractive index, and is shown schematically in Fig. 1. This weak cavity does not significantly change the overall mirror reflectivity but causes a very rapid change of phase on reflection that can lead to significant pulse shaping.

The dispersion of the GTI is determined by the etalon width, and the reflectivity of the front surface. The etalon width is chosen by producing a spacer layer of halfwave stacks of the low refractive index followed by a single quarterwave layer of the high index material. Because such a GTI is based on dichroic coating technology, it is also possible to incorporate additional features into the coating design, such as a pump window. A further advantage of the GTI mirror is that the dispersion can be adjusted by changing the angle of incidence.

The manufacture of GTI mirrors does require stringent control of layer thickness because of the resonant nature of their dispersion curve. Errors in layer thickness may result in both the value and spectral position of the dispersion not meeting the design requirements. Our nominal design was for mirrors having a minimum group delay dispersion (GDD) at 850 nm for an incidence angle of 10°. The coating consisted of 23 alternating quarterwave layers of

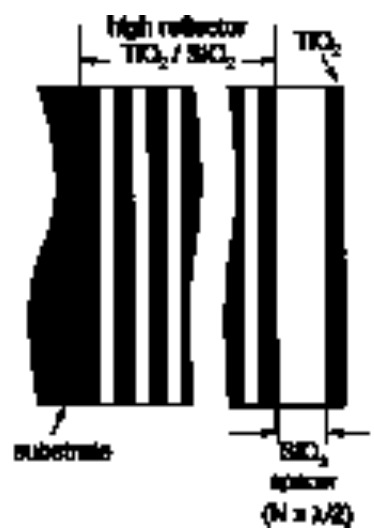

Fig. 1. Design of GTI.

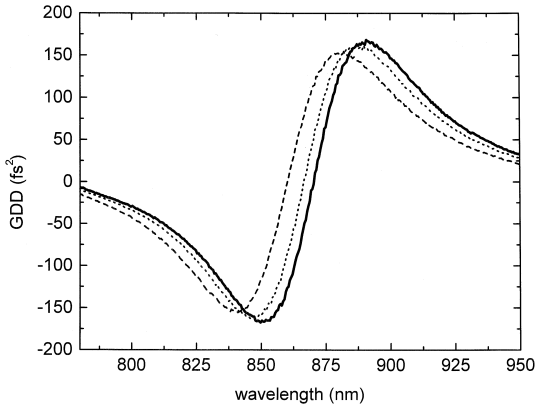

Fig. 2. GDD of GTI (see text). Solid line 0° incidence. Dotted line 9° incidence. Dashed line 15° incidence.

SiO_2 ($n = 1.48$) and TiO_2 ($n = 2.35$) as the high reflector followed by a single halfwave layer of SiO_2 as the spacer and completed with a single quarterwave layer of TiO_2.

The GDD of this design is shown in Fig. 2 for different incident angles. As the angle of incidence is increased, the GDD minimum moves to shorter wavelengths, and the absolute value decreases. Note that it is not possible to move the GDD minimum to longer wavelengths by tuning the angle.

3. Experimental configuration

Fig. 3 shows a schematic diagram of the mode-locked laser configuration investigated. The SBR used in our studies [19] was grown by MOCVD, with a structure similar to that reported in Ref. [8]. We used an astigmatically compensated 'bow-tie' cavity design. The dopant level of the Cr:LiSAF crystal was 3% and each face was Brewster-cut. The crystal was 3 mm long and housed in an aluminium mount. The temperature was stabilised at 15°C by a thermoelectric cooler. The crystal was positioned between two mirrors of 100 mm radius of curvature (ROC). Mirrors M_1, M_2 and M_3 were HR coated ($\geq 99.9\%$) from 820 to 920 nm. Mirror M_3 was used to provide a focus into a SBR, which was simply held onto a copper plate with conducting paste. The incident angle on M_3 was kept as small as possible ($\sim 5°$), and the cavity was completed by a 2.7% output coupler. The folding angle required to compensate the astigmatism due to the crystal was 6.5°. Either one or two plane GTI mirrors could be used for dispersion compensation. The distance between M_1 and M_2 was 107 mm.

The Cr:LiSAF crystal was pumped from both sides by two AlGaInP broad area laser diodes (Polaroid POL-3000 series) rated for 500 mW output power and emitting at ~ 660 nm. The emitter dimension of each diode was 100 μm by 1 μm and each diode package had a μ-lens for collimation in the fast axis. A beam quality measurement of the output from each diode was made, typical values being an $M^2 = 1.4$ in the fast axis and $M^2 = 19$ in the slow axis. The output of each laser diode was then shaped and focused into the crystal using spherical lenses. The spot size (radius) at the focus was measured to be 24 μm by 29 μm for one diode and 24 μm by 36 μm for the other. In order to estimate the amount of power actually available for the pumping process, a 200 μm diameter aperture was positioned at the focus and the power passing through was measured. It was observed that the losses through each lens system (due to transmission and diffraction effects) was 33%, resulting in a maximum available pump power of 660 mW at the crystal. Before using the SBR, we investigated the continuous wave (CW) characteristics of the laser. The CW laser was similar to that of Fig. 3, but without the GTI and with M_3 replaced by a plane HR (without SBR). With this cavity configuration, up to 118 mW of output power was produced using a 2.7% output coupler, the threshold was 81 mW of pump power and the slope efficiency was 16%.

4. Experimental results

Initially a mode-locked cavity containing high quality quartz prisms for dispersion compensation was investi-

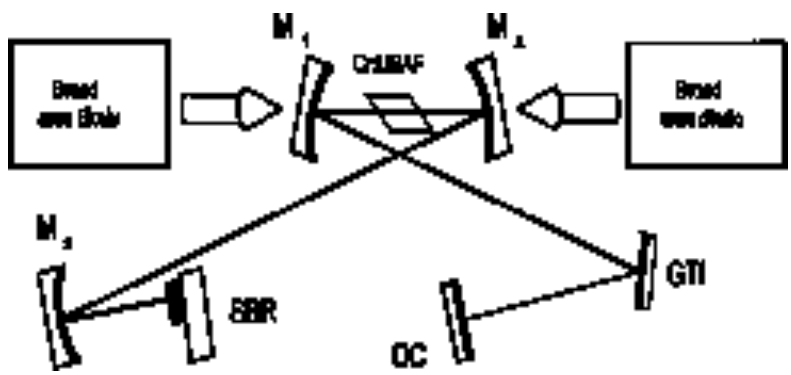

Fig. 3. Schematic of mode-locked laser with a single GTI mirror for dispersion compensation.

gated and characterised for comparison with the prismless cavity. Stable mode-locking occurred with M_3 between ~ 39 to 49 mm from the saturable absorber. Over this range, the estimated spot size in the absorber varied from 54 to 42 μm. Optimum mode-locking occurred for a distance of 44 mm between M_3 and the SBR. The shortest pulse duration observed was 82 fs ($\Delta\lambda = 9$ nm) at a wavelength of 854 nm for a prism separation of 430 mm. The maximum output power observed was 51 mW with a 2.7% output coupler and the repetition rate was 130 MHz. The prisms were then replaced by a single GTI mirror of the design described in Section 2.

Optimum performance was achieved with an incidence angle of 15° on the GTI mirror, providing an estimated minimum GDD of -330 fs^2 for one round trip in the cavity. A typical output curve of the laser is shown in Fig. 4. The CW laser threshold was 160 mW of pump. On steadily increasing the pump power, a point was reached at ~ 570 mW, above which, stable mode-locked operation was self starting. At this point, there was also a jump in laser output power. This can be explained by considering the SBR losses. Below the mode-locking threshold, the SBR exhibits an unsaturated loss of $\sim 1\%$, but when saturated, the losses are reduced, resulting in an increase in output power. Once the self-starting point for mode-locking had been reached, mode-locked operation could still be maintained when there was a subsequent decrease in pump power, as clearly shown in Fig. 4, until a pump power of ~ 460 mW. Below this pump power, no mode-locked behaviour was observed. At pump powers between 460 and 570 mW, stable mode-locking operation could be initiated by an external perturbation.

The maximum power output was 110 mW, indicating that the losses of the GTI mirror were considerably lower than those of the prism pair. Indeed, the mode-locked power in this case is only 7% lower than the maximum

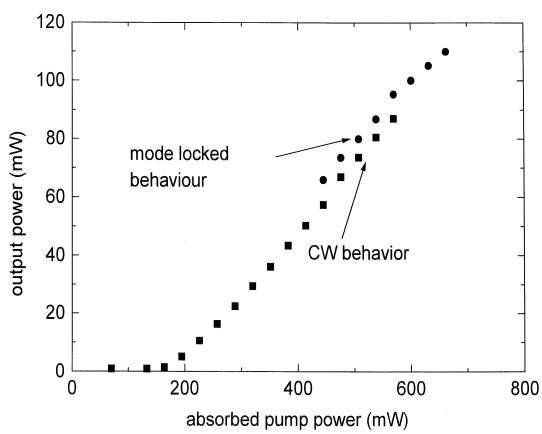

Fig. 4. Output power of the SBR mode-locked laser. The squares indicate purely CW behaviour. The circles indicate mode-locked behaviour.

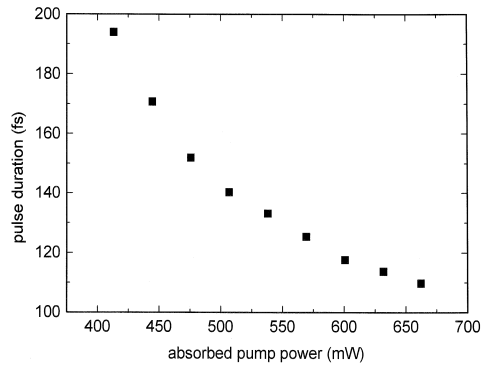

Fig. 5. Pulse duration as a function of absorbed power.

CW power measured with the cavity of only four mirrors. The corresponding pulse duration was 94 fs at 848 nm ($\Delta\lambda = 8.2$ nm). The repetition rate was 130 MHz.

Fig. 5 shows the output pulse duration as a function of absorbed pump power. The pulse duration at the threshold for mode-locked operation is just under 200 fs, and decreases as the pump power is increased. The most likely reason for this behavior is an increase in bandwidth due to enhanced levels of self phase modulation for higher intracavity powers, leading to the generation of shorter pulses. Furthermore, such behaviour can be predicted from the soliton mode-locking model [20].

Of further interest is the performance of the laser for different incident angles on the GTI. For this measurement, the diodes were run at maximum pump power. The pulse duration and centre wavelength for incident angles of 9°, 11°, 13.5°, and 15° is shown in Fig. 6. The results are also shown in Table 1. It can be seen that both the pulse duration and central wavelength of the laser decreased as the incident angle was increased. This reduction of the pulse duration was due to the change in GDD with incidence angle.

It was not possible to have incident angles less than 9° because of the physical dimensions of the experimental

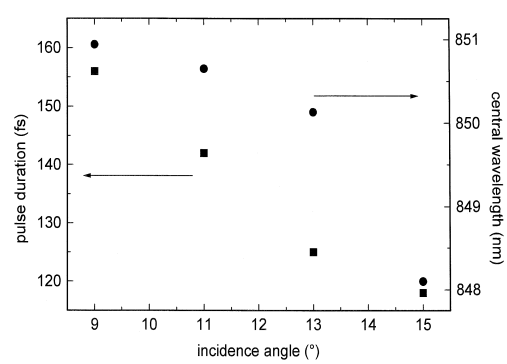

Fig. 6. Pulse duration (squares) and central wavelength (circles) as a function of incidence angle on the GTI.

Table 1
Performance of mode-locked laser as GTI incidence angle is changed

Angle	Centre wavelength (nm)	GDD (fs^2)	Pulse duration (fs)	Power (mW)
9°	851.0	−374	156	82
11°	850.5	−362	142	84
13°	850.0	−330	125	85
15°	848.0	−328	118	80

setup. There was no mode-locking for angles greater than 15°, due to the fact that the wavelength of the dispersion minimum had moved too far from the wavelength of operation possible for the SBR which was designed for operation at 850 nm, to coincide with the gain maximum of Cr:LiSAF. For this reason, it was not possible to achieve the same minimum pulse duration as with prisms. To achieve the same minimum pulse duration would require a slight change in the GTI design in order to decrease the absolute amount of negative GDD at the operating wavelength of the SBR. Alternatively, one could increase the amount of positive dispersion by the insertion of a piece of glass into the cavity.

Finally, to assess the stability of the mode-locked pulse train, we measured both the phase and amplitude noise characteristics of the output using the technique of power-spectrum measurement as described in Ref. [21]. In our measurement, we used a 25 GHz photodetector (New Focus Model 143X) and a microwave spectrum analyser with a frequency range up to 2.6 GHz (Advantest R3261A). The laser was operating with optimum performance at a repetition rate of 130 MHz. We measured the power-spectra of the fundamental and twenty fifth harmonics of the laser cavity frequency with resolution bandwidths of 30 Hz, 100 Hz, and 1 kHz depending on the range of frequency offsets. The single-sideband phase- and amplitude noise spectra are shown in Fig. 7(a) and (b). The rms timing jitters and amplitude noise figures were calculated in three frequency ranges, 100–500 Hz, 500–5000 Hz, and 5–50 kHz. The results are presented in Table 2 and indicate that the laser exhibits low noise characteristics.

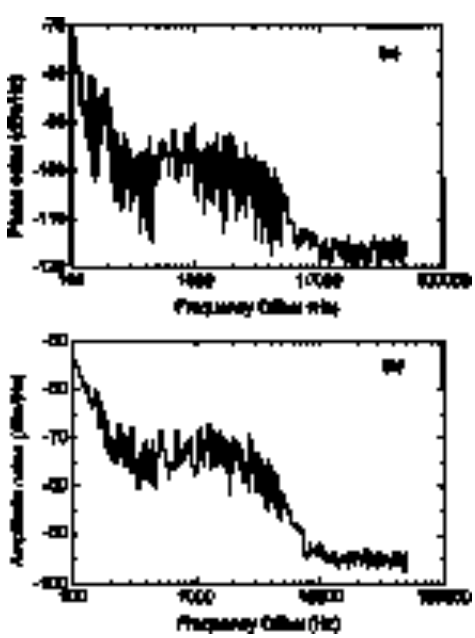

Fig. 7. (a) Single side-band phase noise spectral density and (b) single side-band amplitude noise spectral density of the SBR mode-locked Cr:LiSAF laser.

Table 2
Phase noise (timing jitter) and amplitude noise characteristics of the SBR mode-locked Cr:LiSAF

Frequency range	Phase noise	Amplitude noise
100–500 Hz	1460 fs	1.5%
500–5000 Hz	1240 fs	1.7%
5–50 kHz	630 fs	0.5%

5. Conclusions

In conclusion, we have demonstrated a diode pumped, SBR mode-locked femtosecond laser with a single GTI mirror for dispersion compensation, producing pulses as short as 94 fs and an average output power of up to 110 mW. The use of only a single GTI for dispersion compensation resulted in low overall cavity losses, increasing the total available mode-locked output power as compared to a prism based system. Furthermore, the advantage afforded by folding the cavity through the use of GTI mirrors as dispersion compensating elements resulted in a compact design, with the complete laser system, including pump lasers, having a footprint of only 60 cm by 30 cm. The use of an SBR ensured that the mode-locking was stable and self-starting.

This simple, compact femtosecond oscillator has been used successfully for the last 6 months as a source for producing THz radiation, replacing an existing argon-ion pumped, femtosecond Ti:sapphire laser. As well as saving valuable space on the optical table, the system requires no warm-up time and has proven easy to use and maintain.

Acknowledgements

The authors would like to thank Christoph Becher for valuable discussions regarding noise measurements.

References

[1] D.M. Mittleman, S. Hunsche, L. Boivin, M. Nuss, Opt. Lett. 22 (1997) 904.
[2] G. Robertson, D. Armstrong, M.J.P. Dymott, A.I. Ferguson, Appl. Opt. 36 (1997) 2481.
[3] B. Bouma, G.J. Tearney, I.P. Bilinsky, B. Golubovic, J.G. Fujimoto, Opt. Lett. 21 (1996) 1839.
[4] S.A. Payne, L.L. Chase, L.K. Smith, W.L. Kway, H.W. Newkirk, Appl. Phys. 66 (1989) 1051.
[5] L.K. Smith, S.A. Payne, W.L. Kway, B.H. Chai, IEEE J. Quantum Electron. 28 (1992) 2612.
[6] M.J.P. Dymott, A.I. Ferguson, Opt. Lett. 20 (1995) 1157.
[7] D. Kopf, K.J. Weingarten, L. Brovelli, M. Kamp, U. Keller, Opt. Lett. 22 (1994) 2143.
[8] S. Tsuda, W.H. Knox, E.A. de Souza, W.Y. Jan, J.E. Cunningham, Opt. Lett. 20 (1995) 1406.
[9] A. Robertson, R. Knappe, R. Wallenstein, Opt. Commun. 147 (1998) 294.
[10] D. Kopf, A. Prasad, G. Zhang, M. Moser, U. Keller, Opt. Lett. 22 (1997) 621.
[11] F. Gires, P. Tournois, C. R. Acad. Sci. Paris 258 (1964) 6112.
[12] R. Szipöcs, A. Köházi-Kis, Appl. Phys. B 65 (1997) 115.
[13] J. Kuhl, M. Serenyi, E.O. Göbel, Opt. Lett. 12 (1987) 334.
[14] J. Heppner, J. Kuhl, Appl. Phys. Lett. 47 (1985) 453.
[15] I.T. Sorokina, E. Sorokin, E. Winter, A. Cassanho, H.P. Jenssen, R. Szipöcs, Appl. Phys. B 65 (1997) 245.
[16] K. Gäbel, P. Russbüldt, R. Lebert, P. Loosen, R. Poprawe, A. Valster, Conference on Lasers and Electro-Optics Europe '98, Optical Society of America, Washington, DC, 1998, paper CtuM39.
[17] D. Kopf, G. Zhang, R. Fluck, M. Moser, U. Keller, Opt. Lett. 21 (1996) 486.
[18] K. Gäbel, P. Rußbüldt, R. Lebert, P. Loosen, R. Poprawe, H. Heyer, A. Valster, Opt. Commun. 153 (1998) 275–281.
[19] D. Burns, S.T. Lee, M.D. Dawson, A.I. Ferguson, Conference on Lasers and Electro-Optics '97, Optical Society of America, Washington, DC, 1997, paper CTuP39.
[20] F.X. Kärtner, I.D. Jung, U. Keller, IEEE J. Sel. Top. Quantum Electron. 2 (1996) 540.
[21] D. von der Linde, Appl. Phys. B 39 (1986) 201.